Sensors & Actuators: B. Chemical 376 (2023) 132985

Contents lists available at ScienceDirect

Sensors and Actuators: B. Chemical

journal homepage: www.elsevier.com/locate/snb

Porous hydrogel scaffolds integrating Prussian Blue nanoparticles: A versatile strategy for electrochemical (bio)sensing

Roberto Baretta [a,1], Ada Raucci [b,1], Stefano Cinti [b,c,*], Marco Frasconi [a,**]

[a] Department of Chemical Sciences, University of Padova, Via Marzolo 1, 35131 Padova, Italy
[b] Department of Pharmacy, University of Naples Federico II, 80131 Naples, Italy
[c] BAT Center, Interuniversity Center for Studies on Bioinspired Agro-Environmental Technology, University of Napoli Federico II, 80055 Naples, Italy

ARTICLE INFO

Keywords:
Amperometric sensors
Cellulose
Screen-printed electrodes
Hydrogel films
Ethanol
Glucose

ABSTRACT

Hydrogels have emerged as promising porous soft materials from which to develop a wide range of biosensing platforms due to the possibility to easily engineer their properties and to effectively immobilize enzymes and nanomaterials in their matrix. Despite their attractive properties, the ability to form stable hydrogel films integrating well–dispersed catalytic nanomaterials and enzymes on electrode surfaces is still required to enable their implementation into electrochemical biosensors. Here, we report a facile approach to prepare hydrogel films embedding Prussian Blue nanoparticles (PBNPs) and different enzymes on electrode surfaces for electrochemical biosensing. A one-pot strategy was employed for the synthesis, under mild conditions, of PBNPs and the simultaneous immobilization of enzymes in a highly functionalized carboxymethyl cellulose matrix, yielding homogeneous hydrogel composites. Highly porous hydrogel films were successfully prepared by drop casting the hydrogel composites on the surface of flexible screen–printed electrodes (SPEs). Due to the high loading of well–dispersed PBNPs, the hydrogel films demonstrated good electrocatalytic activity for both the oxidation of NADH and the reduction of hydrogen peroxide resulting in high detection sensitivity. Two amperometric biosensors for the rapid detection of glucose and ethanol in serum were realized by employing hydrogel composites integrating glucose oxidase and alcohol dehydrogenase. By combining the unique features of hydrogels on flexible electrochemical strips, our approach holds great promise for the development of portable electrochemical (bio)sensors, which are easy to fabricate and versatile for the detection of a variety of analytes.

1. Introduction

The continuous search of materials for sensors development is based on the achievement of enhanced sensing performances combined to the sustainability and robustness of the device. There is an increasing interest to simplify the fabrication of biosensors, which can be obtained from cheap, nontoxic or biocompatible materials, prepared following the principles of green chemistry, avoiding hazardous procedures and expanding the range of applications towards wearable and non–invasive measurements [1,2].

Hydrogels are attractive materials for the development of biosensors because they combine all those features in a water–rich polymer network [3]. Indeed, hydrogels are highly versatile soft materials as their properties can be readily engineered from the molecular level, e.g. the soft and flexible scaffold of hydrogels can be toughened by physical or chemical crosslinking. Hydrogels can be obtained from natural polymers, such as cellulose derivatives [4], acting as gelators, crosslinked under biocompatible conditions and they can be designed to respond to different external stimuli such as light, temperature, pH and different molecules [5]. Therefore, they are attracting a tremendous interest as functional components of actuators and sensors [6,7]. When they are used in the context of bioanalytical assays and biosensing, the target analyte can easily permeate through the 3D matrix of the hydrogel because of its high porosity [8]. Indeed, the reticulated hydrophilic polymer chains can absorb a high amount of water leading to a volumetric expansion of the hydrogel and generating a microporous structure [9]. In addition, nanometer–sized pores are formed between the crosslinked polymeric chains, allowing the immobilization of enzymes

* Corresponding author at: Department of Pharmacy, University of Naples Federico II, 80131 Naples, Italy.
** Corresponding author.
E-mail addresses: stefano.cinti@unina.it (S. Cinti), marco.frasconi@unipd.it (M. Frasconi).
[1] These authors equally contributed.

https://doi.org/10.1016/j.snb.2022.132985

Available online 12 November 2022

and nanoparticles (NPs), which confer to the hydrogel desired selectivity for the analyte and catalytic, plasmonic or conductive properties. Thus, hydrogel composite materials obtained by combining the properties of porous polymeric networks and the plasmonic properties of NPs have been employed for optical sensing [10], while conductive hydrogels have been developed for electrochemical sensing by integrating metal NPs or conductive polymers in the hydrogel matrix [11,12].

Prussian Blue (PB), which is a metal organic framework based on ferric ferrocyanide, is without any doubt one of the most versatile and efficient catalytic nanomaterials to be coupled with the world of sensors and biosensors [13–16]. From a catalytic point of view, Prussian Blue has been defined as an "artificial peroxidase" [17], because of its ability to reduce hydrogen peroxide. Therefore, Prussian Blue has been combined with oxidase enzymes to detect glucose, cholesterol, lactate and ethanol through electrochemical readout [18–21], including the development of self–powered wearable sensors [22,23]. Prussian Blue nanoparticles (PBNPs), due to their porous structure, display high and versatile catalytic activity allowing the electrocatalytic reduction and oxidation of a broad class of analytes [24]. In particular, PBNPs have high selectivity and sensitivity towards the reduction of hydrogen peroxide, which is the by–product of oxidase enzymes, and also to oxidize NADH, which is the by–product of dehydrogenase enzymes. Therefore, the application of oxidative or reductive electrochemical potentials can switch the sensitivity of PBNPs between those clinically relevant species [25].

An increasing interest and importance is raising for the development of all–in–one biosensor fabrication approach with high sensibility, stability, eco–compatibility and easiness of application on diverse substrates, as the electrochemical strips. In most of the examples reported in literature for the fabrication of electroanalytical biosensing architectures, multiple steps are required, including the step–by–step combination of electrochemical mediators, physically or chemically trapped, and enzymes. For the specific case of PB, several methods have been reported for the preparation of PB–based electrochemical biosensors [26], but each one displays intrinsic problems related to the reactions involved for the immobilization of enzymes on electrodes and for the stability of PB, especially in the form of NPs. PBNPs are commonly prepared by coprecipitation method using different capping agents, including citrate [27] or polymer chains, such as polyvinyl pyrrolidone [28], but the reaction conditions are not compatible with the presence of enzymes, that are coupled with PBNPs to fabricate biosensors. In fact, high temperature or organic solvents are employed in order to control the shape and diameter of PBNPs [28]. PBNPs can also be grown directly on the electrode upon application of an electrochemical potential in acidic solutions [26]. However, also these reaction conditions cannot be applied for the concomitant immobilization of enzymes.

Mild and biocompatible conditions must be employed for the generation of PBNPs and the simultaneous immobilization of the active enzyme, thus avoiding the enzyme denaturation from high temperatures or harsh reagents. Hydrogels represent a unique scaffold to control the growth of the NPs under mild reaction conditions, i.e. at room temperature and in water solutions, preventing also the aggregation of NPs. A green method for the synthesis of PBNPs has been reported by using a microporous carboxymethyl cellulose nanofibrils membrane to control the growth of the NPs [29]. The developed approach, however, precludes the possible immobilization of enzymes because it comprises an initial formation of a highly crosslinked network between cellulose chains and Fe^{3+}, a precursor for PBNPs synthesis. Therefore, a one–pot approach for the synthesis of PBNPs is essential for an effective immobilization of enzymes within the hydrogel, which otherwise can hardly permeate through the smaller pores of the hydrogel network once they are formed. Recently, we developed a facile method for the templated synthesis of PBNPs and the immobilization of enzymes by using an hydrogel scaffold based on carboxymethyl cellulose (CMC) [30], a cellulose derivative with carboxymethyl groups. The CMC matrix acts as templating agent for the controlled growth of the PBNPs and as gelator for the generation of the hydrogel network, resulting also in the immobilization of the enzymes. The obtained hydrogel composite with embedded enzymes has been applied for the colorimetric detection of glucose. An attractive feature of CMC–based hydrogels as biosensor interfaces is their ability to reduce the nonspecific adsorption of proteins from blood and biofluid samples due to the swelling of the polysaccharide chains [31]. Despite the promising properties of aqueous dispersions of these hydrogel composites, the ability to form stable hydrogel films on different surfaces is still required to enable their integration into robust electrochemical biosensing devices.

Using the green hydrogel–based strategy as starting point, here we demonstrate a facile and versatile fabrication of stable PBNPs–CMC hydrogel films embedding different enzymes on electrode surfaces for electrochemical biosensing (Fig. 1). The formation of stable composite hydrogel films, avoiding the leakage of NPs and enzymes, is achieved by employing a polymer matrix based on CMC with a higher content of carboxymethyl groups compared to our previous report [30]. Moreover, the approach developed in this work enables to prepare hydrogel composites with smaller PB particles size and highly crosslinked network. We demonstrated that the hydrogel films obtained from this fabrication approach are well suited for electrochemical biosensing because they display an enhanced stability of the embedded PBNPs during their redox cycling, resulting in enhanced electrocatalytic currents, and they preserve the catalytic activity of the immobilized enzymes, glucose oxidases (GOx) and alcohol dehydrogenase (ADH), on the electrode surface. Therefore, by modifying the working electrode of flexible screen–printed electrodes (SPEs) with a film of these composite hydrogels, highly stable electrochemical biosensors for the detection of NADH, ethanol and glucose were obtained. The high stability and detection performance of the developed electrochemical biosensors are achieved by combining the unique features of hydrogels with the flexible SPE substrates. Indeed, the flexibility of the hydrogel film and the SPE substrate allows the formation of homogeneous films adhering on the conductive surface of the electrode, while the porous structure of the hydrogel provides a highly permeable matrix for small analytes.

The possibility to detect different analytes by these hydrogel–based (bio)sensors can be easily achieved thanks to the versatility of the procedure for the preparation of the hydrogel films. Therefore, our approach holds great promise for the development of novel architectures due to the ease of preparation of the composite hydrogel in biocompatible reaction conditions from renewable sources, providing a porous scaffold for the immobilization of different enzymes, that will ultimately lead to highly versatile (bio)sensing platforms.

2. Experimental section

2.1. Reagents and materials

Sodium carboxymethyl cellulose (NaCMC, M.W. 250 kDa) with degree of substitution (DS) of 0.9 and 1.2, potassium hexacyanoferrate(II) trihydrate ($K_4[Fe(CN)_6]\cdot 3\,H_2O$, 98.5 %), glucose oxidase from *Aspergillus Niger* (GOx, 145 U/mg), alcohol dehydrogenase from *Saccharomyces cerevisiae* (ADH, 296 U/mg), iron(III) nitrate nonahydrate ($Fe(NO_3)_3\cdot 9\,H_2O$, 98 %), 30 % (w/w) hydrogen peroxide (H_2O_2) solution, potassium phosphate monobasic (>99 %), potassium chloride (KCl), potassium hydroxide (>85 %), β–nicotinamide adenine dinucleotide disodium salt hydrate, reduced form (NADH, >97 %), β-nicotinamide adenine dinucleotide hydrate (NAD^+, >96 %), *N*–(2–Hydroxyethyl) piperazine–*N*'–(2–ethanesulfonic acid) (HEPES, >99.5 %), and human serum were all purchased from Sigma Aldrich Co. (St. Louis, MO).

2.2. Apparatus

Scanning electron microscopy (SEM) with energy dispersive X–ray spectroscopy (EDX) images were taken on a Zeiss Sigma HD microscope, equipped with a Schottky FEG source, one detector for backscattered

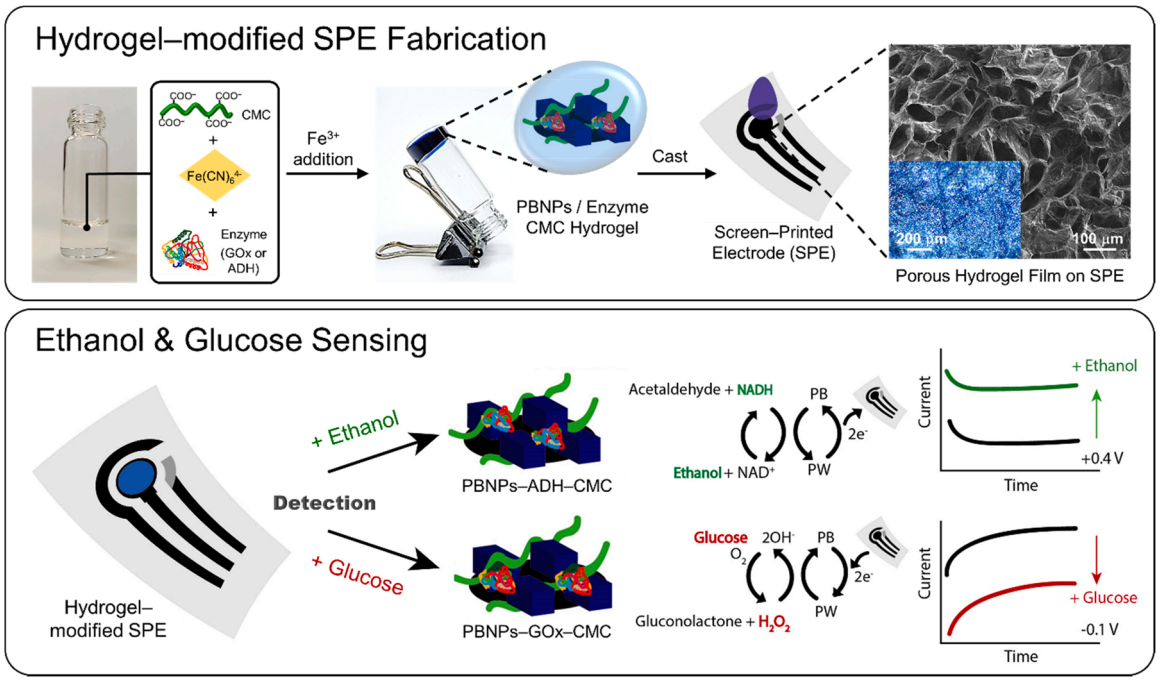

Fig. 1. (Top) Schematic representation of hydrogel composites preparation through the *in–situ* synthesis of PBNPs in the CMC matrix in the presence of the enzyme (GOx or ADH). The formation of the hydrogel composite is confirmed by the tube inversion test (central photo). The modification of flexible screen–printed electrodes (SPE) with the hydrogel composite results in an effective porous film on the electrode surface as confirmed by SEM image and optical microscopy image (inset) of PBNPs–CMC hydrogel. (Bottom) Operation principle of the ethanol biosensor based on the electrocatalytic oxidation of NADH generated by the ADH–mediated oxidation of ethanol on the PBNPs-ADH-CMC modified SPE and of the glucose biosensor based on the electrocatalytic reduction of H_2O_2 generated by the GOx–mediated oxidation of glucose on the PBNPs–GOx–CMC modified SPE.

electrons and two detectors for secondary electrons (InLens and Everhart Thornley). Transmission electron microscopy (TEM) images were taken on a Tecnai G^2 (FEI) operating at 100 kV. Images were captured with a Veleta (Olympus Soft Imaging System) digital camera. Ultraviolet–visible (UV–vis) spectra were collected using an Agilent Cary 60 spectrophotometer. X–Ray diffraction patterns were recorded on a Bruker D8 ADVANCE Plus Diffractometer in Brag–Brentano geometry employing Cu Kα line radiation. All electrochemical measurements were carried out by a EmStat^3 (PalmSens, The Netherlands).

2.3. Preparation of PBNPs–CMC

The synthesis of PBNPs–CMC hydrogel composites was performed according to a previous procedure with some modification [30]. In particular, a matrix of CMC with DS 1.2 was chosen for this work. Briefly, NaCMC (DS 1.2) (120.0 mg) was dissolved homogeneously in deionized water (6.0 ml) and after the addition of a solution of $K_4[Fe(CN)_6]\cdot 3H_2O$ (150 mM, 300 µl), a pale–yellow homogeneous solution is obtained. Subsequently, the dropwise addition of a solution of $Fe(NO_3)_3\cdot 9H_2O$ (10 mM, 6.0 ml) at the rate of 0.5 ml/min under vigorous magnetic stirring causes the formation of a blue suspension, which was kept under stirring continuously for 5 min at room temperature. In order to obtain homogeneous and monodisperse PBNPs in the CMC–based hydrogel, the optimal concentrations of the reagents in the mixture were 1 % w/w of CMC (DS 1.2), 3.75 mM of $[Fe(CN)_6]^{4-}$ and 5 mM of Fe^{3+}. The reaction mixture was washed with 3.0 ml of water and centrifugated for 3 min at 8300 rpm. After the removal of the supernatant, the collected blue hydrogel was redispersed in 5.0 ml of deionized water and stored at 4 °C.

2.4. Preparation of enzyme–loaded PBNPs–CMC

The synthetic procedure for the preparation of the composite hydrogel integrating the PBNPs and the enzyme (GOx or ADH) is similar to the above mentioned. For the synthesis of PBNPs–GOx–CMC hydrogel, in the 6.0 ml solution of CMC (DS 1.2) 1 % w/w and $[Fe(CN)_6]^{4-}$ 3.75 mM, 300 µl of GOx solution 6 mg/ml were added. Then, after the dropwise addition of 6.0 ml of Fe^{3+} 10 mM solution under vigorous magnetic stirring, the blue reaction mixture is diluted with 3.0 ml of DI water. The mixture was centrifugated for 3 min at 8300 rpm and the collected blue hydrogel redispersed in 10.0 ml of DI water and stored at 4 °C. For the synthesis of PBNPs–ADH–CMC hydrogel, in the 6.0 ml solution of CMC (DS 1.2) 1 % w/w and $[Fe(CN)_6]^{4-}$ 3.75 mM, 300 µl of ADH solution 9 mg/ml were added, and the subsequent steps of dropwise addition of Fe^{3+}, dilution, centrifugation, redispersion and storage were the same as for PBNPs–GOx–CMC hydrogel.

2.5. Fabrication of screen–printing electrodes (SPE)

Screen–printed electrodes have been manufactured by serigraphy. Autostat HT5 polyester sheets were used as the flexible support. Ag/AgCl (Elettrodag 477 SS) ink has been used to print the reference electrode, while graphite-based conductive ink (Elettrodag 421) has been used for printing both the working and counter electrode [32]. After each printing steps, the electrodes have been cured in the oven for 20 min at 80 °C. The area of the electrochemical cell has been defined by using an adhesive tape also avoiding samples reaching the electrical connectors at the potentiostat. The final diameter of the working electrode is 4 mm.

2.6. Hydrogel–modified SPE fabrication

All the electrodes have been modified through the adoption of a drop casting procedure. For the optimization of the sensing performance, different volumes of hydrogels were used for the fabrication of the films on the electrodes. The modification was performed by adding 2 µl of hydrogel stepwise onto the working electrode surface until the final volume of 2, 4, 6 or 8 µl was reached. Prior to be used for sensing

applications, the modified electrodes were stored overnight at 4 °C.

2.7. Hydrogen peroxide, glucose, NADH, and ethanol detection

Chronoamperometry was used for hydrogen peroxide, glucose, NADH and ethanol detection on the modified electrodes. In particular, NADH was detected by the PBNPs–CMC modified SPE using an applied potential of 0.4 V (vs. Ag/AgCl). Ethanol was indirectly quantified by measuring the by–produced NADH by the PBNPs–ADH–CMC modified SPE, using an applied potential of 0.4 V (vs. Ag/AgCl). Glucose was indirectly quantified by measuring the by–produced hydrogen peroxide by the PBNPs–GOx–CMC modified SPE, using an applied potential of −0.1 V (vs. Ag/AgCl). The calibration curves were obtained from three repetitions using different electrodes. The detection limit for the different analytes has been calculated using the following approximation, i.e. three times the standard deviation of the blank solution divided by the slope of the calibration curve. The mean repeatability of the method was calculated by considering the relative standard deviation (RSD) due to three replicates.

3. Results and discussion

3.1. Preparation and characterization of hydrogel–modified SPEs

The PBNPs-CMC composite was prepared according to the hydrogel-based strategy previously reported [30], but modified by using CMC with a high degree (1.2) of substitution of the carboxymethyl groups on the cellulose chains in order to obtain hydrogel films on electrodes with enhanced mechanical characteristics and sensing performances. The PBNPs-CMC composite hydrogel was prepared in one pot by dropwise addition of a 5 mM Fe^{3+} solution to a solution of CMC (DS 1.2) at 1% w/w in the presence of 3.75 mM of $[Fe(CN)_6]^{4-}$ under vigorous stirring. The formation of PBNPs induces the immediate gelation of the CMC solution resulting in a blue PBNPs—CMC hydrogel, as confirmed by the tube inversion test (Fig. 1). On the contrary, the addition of Fe^{3+} ions on a CMC solution without $[Fe(CN)_6]^{4-}$ results in the formation of an orange hydrogel (Fig. S1A), due to the coordination between the carboxylic groups of CMC and the Fe^{3+} ions [33]. The addition of Fe^{3+} ions into an aqueous solution of $[Fe(CN)_6]^{4-}$ without CMC results instead in the precipitation of Prussian Blue aggregates (Fig. S1B), which is a ferric ferrocyanide redox active metal organic framework [34]. When the reaction of Fe^{3+} with $[Fe(CN)_6]^{4-}$ was performed in the confined environment of an hydrated network of CMC, an homogeneous blue CMC—based hydrogel crosslinked by Prussian Blue nanoparticles formed. Well dispersed PBNPs are obtained from direct reaction between Fe^{3+} and $[Fe(CN)_6]^{4-}$ in the CMC matrix, which influences the crystallization of PBNPs and controls their growth. The resulting PBNPs are stabilized by the CMC chains through the coordination between the carboxylate groups of CMC and the positively charged iron centers on the surface of the PBNPs. This crosslinking network is the responsible for the formation of the hydrogel composite at the end of the reaction. Therefore, the presence of the CMC matrix not only controls the nucleation during the reaction and the size of PBNPs, but also prevents the formation of aggregates by acting as capping agent of the NPs.

In order to demonstrate the versatility of our synthetic approach for the preparation of the PBNPs hydrogel composites for the fabrication of biosensors, we have prepared PBNPs-CMC hydrogels in the presence of the enzymes GOx and ADH, which are commonly used in combination with Prussian Blue for the development of glucose and ethanol biosensors, respectively. The addition of a solution of Fe^{3+} ions on a solution containing CMC and $[Fe(CN)_6]^{4-}$ in presence of enzymes results in the formation of a well–dispersed and homogeneous blue hydrogel. This approach simplifies the procedure for the preparation of integrated PB/enzyme systems needed for the fabrication of biosensors as the GOx or ADH are immobilized in the hydrogel matrix during the synthesis of the PBNPs, resulting in a more uniform distribution of enzymes and NPs. All prepared hydrogel composites, PBNPs-CMC, PBNPs-GOx-CMC and PBNPs-ADH-CMC, were swelled in water solution and washed with phosphate buffer to completely remove unreacted chemicals and non–entrapped enzymes. With our hydrogel composites, electrochemical (bio)sensors for NADH, ethanol and glucose can be simply prepared by dropping the PBNPs-CMC, PBNPs-ADH-CMC and PBNPs-GOx-CMC, respectively, on the surface of screen–printed electrodes.

Optical microscopy images of the composite film on the electrode surface display an homogeneous distribution of the blue film without cracks suggesting the successful preparation of the modified SPE. The hydrogel films deposited on the SPEs were then characterized by scanning electron microscopy (SEM). The SEM images of the PBNPs-CMC composite film displays a microporous structure with regular pores ranging between 70 and 100 μm (Fig. 1), similar to those observed for other CMC—based hydrogels [35]. The porous structure of lyophilized hydrogel composites loaded with the enzyme (Fig. S2) shows comparable pore shape and size with the PBNPs-CMC composite hydrogel. Thus, the presence of enzymes in the reaction mixture does not alter the microporous structure of the hydrogel composites. Furthermore, the highly porous nature of the prepared hydrogel films facilitates the diffusion of analytes and products of the enzymatic reactions to the electrode surface.

The composition of the hydrogel film on the electrode surface was determined by EDX elemental analysis. The EDX spectrum of PBNPs-CMC displays (Fig. 2A) the presence of Na, C, and O from CMC and of Fe, K, and C from the Prussian Blue NPs. From the EDX mapping, a homogeneous distribution of Fe and K can be observed in the sample, demonstrating that PBNPs are formed inside the hydrogel network and they are homogeneously dispersed in the polymer matrix. The EDX elemental analysis and mapping of enzyme–loaded PBNPs–CMC composite displays (Fig. S3) the same elements, from cellulose and PBNPs, further indicating that the formation of PBNPs homogeneously dispersed in the cellulose matrix is unaffected by the presence of enzymes.

The formation of well–dispersed nanostructures of PB is confirmed also by TEM images (Fig. 2B and S4), in which the cubic shapes of PBNPs [36] are distributed in the hydrogel matrix and no aggregates can be observed. From the TEM images, it is possible to determine the size distribution of the NPs, which ranges from 10 to 20 nm; by fitting with the log–normal distribution function, an average size of 15 nm is obtained. For comparison, the previous reported approach for the preparation of PB–CMC hydrogel composite [30], where CMC with a lower content of carboxymethyl groups (DS 0.9) was employed, provided PBNPs with an average size of 21 nm. The smaller size of the PBNPs obtained here can be ascribed to the higher content of carboxylate groups on the CMC, resulting in a higher coordination of the PBNPs during their growth. This result demonstrates that the size of the PBNPs can be easily tuned by using CMC with different degrees of substitution, lending further support to the templating effect of the CMC matrix during the synthesis of PBNPs.

Crystallographic insight into the formation of PBNPs in the CMC matrix was obtained via powder X-ray diffraction (PXRD). The diffraction patterns of air–dried PBNPs–CMC and PBNPs–GOx–CMC composites display (Fig. S5) the same peaks, located at 17.5°, 24.8°, 35.3°, 39.6°, 43.6°, 50.7°, 54.0°, 57.2°, 66.2° and 68.9°, which are typical of crystalline Prussian Blue [37–39]. This result demonstrates that the presence of enzymes during the synthesis of PBNPs in the CMC matrix does not affect the crystallinity of the resulting PBNPs.

The prepared PBNPs–CMC hydrogel composites can be easily drop casted on different substrates, such as glass, metals and carbon surfaces, to form homogeneous hydrogel films. UV–vis spectra of PBNPs–CMC and enzyme–loaded PBNPs–CMC hydrogels deposited on quartz slides display (Fig. 3A) an absorption band centered at 685 nm, typical of PBNPs [40]. The spectra of the hydrogel composites with and without the enzymes show the same absorbance values, indicating that the same amount of PBNPs is embedded in the different hydrogel composites.

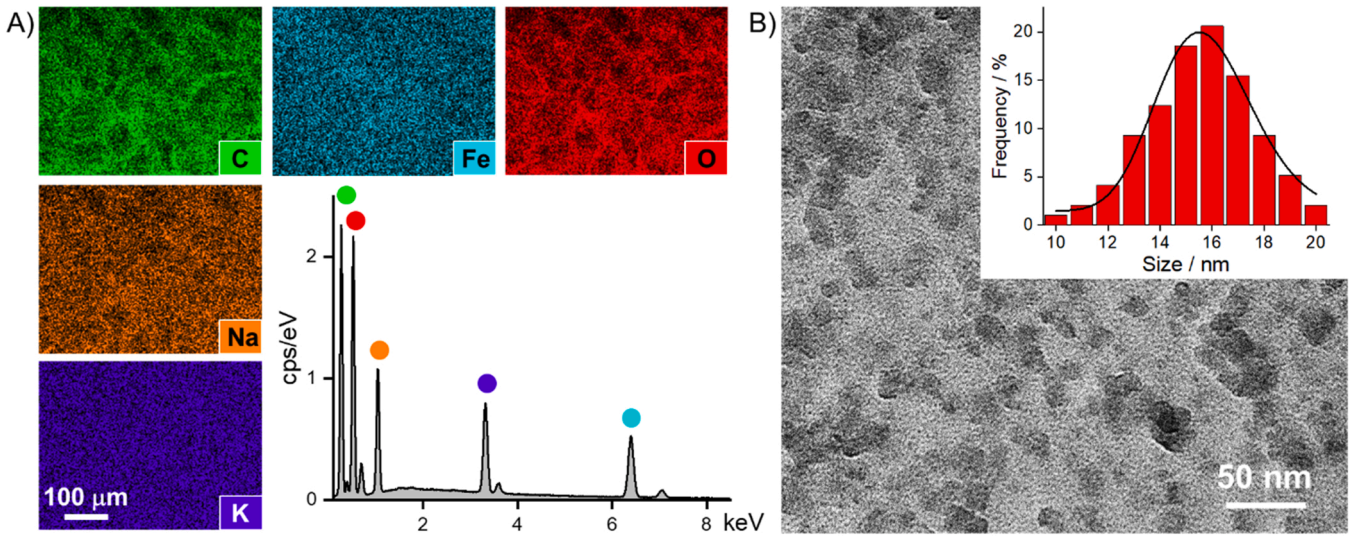

Fig. 2. A) EDX spectrum and EDX mapping images of PBNPs–CMC hydrogel film on SPE. B) TEM image of PBNPs–CMC hydrogel and size distribution (inset) of the PBNPs growth in the CMC hydrogel.

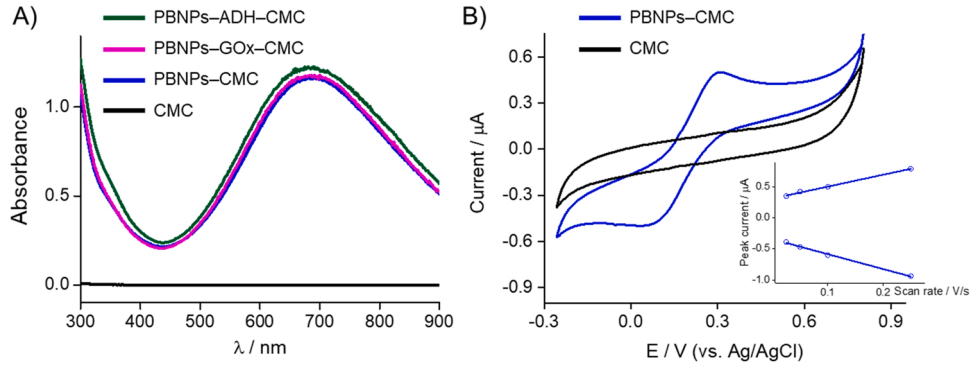

Fig. 3. A) UV–vis spectra of CMC (black), PBNPs–CMC (blue), PBNPs–GOx–CMC (pink) and PBNPs–ADH–CMC (dark green) films on quartz slides. B) Cyclic voltammograms of PBNPs–CMC (blue) and CMC (black) films on SPE (scan rate: 50 mV/s). Inset: Variation of the anodic and cathodic peak current vs. scan rate for the PBNPs–CMC modified SPE.

The electrochemical properties of the PBNPs–CMC hydrogel were investigated by drop casting the hydrogel on an electrode surface. The cyclic voltammogram of a film of PBNPs–CMC on a SPE shows a couple of quasi-reversible peaks due to the Prussian Blue/Prussian White redox process (Fig. 3B and S6), which is absent in the voltammogram of a CMC film on SPE. The formal potential determined for the redox process is 0.190 V (vs Ag/AgCl), in agreement with the redox potential values reported for other PBNPs immobilized on electrode surfaces [41,42]. The linear dependence of anodic and cathodic peak currents with the potential scan rate reveals the typical behavior of a non–diffusive specie, indicating that PBNPs are immobilized in the hydrogel matrix, where they crosslinked the CMC chains. From the slope of the lines we determined the surface coverage of electrochemically active centers of the PBNPs–CMC hydrogel-coated electrode [43], which is 4.5 pmol/cm^2.

Therefore, the synthetic approach developed here provides a facile one–pot strategy for the preparation of well-dispersed PBNPs embedded in a highly crosslinked cellulose–based hydrogel. These results demonstrated that the CMC chains with a high degree of substitution of carboxymethyl groups act as (i) templating agent for the synthesis of crystalline PB yielding NPs with narrow distribution of sizes and (ii) scaffold for the formation of an highly crosslinked hydrogel with embedded PBNPs. Moreover, the developed procedure is versatile for the fabrication of electrochemical biosensors, owing to the possibility to entrap enzymes in the hydrogel composite during the preparation of the PBNPs in one–pot approach, without affecting the properties of the PBNPs.

3.2. *Hydrogen peroxide and glucose sensing*

Our approach for the fabrication of porous and flexible electrochemical biosensing platforms by employing the developed hydrogel composites takes advantages of the properties of highly functionalized cellulose–based hydrogels to form homogeneous films on substrates of different materials. Therefore, PBNPs–CMC, PBNPs–ADH–CMC and PBNPs–GOx–CMC hydrogel composites have been applied in combination with flexible screen–printed electrodes towards the development of portable electrochemical biosensors for the detection of NADH, ethanol and glucose, respectively. It should be noted that the fabrication of modified SPEs with robust hydrogel films containing PBNPs opens to wide possibility towards the development of portable diagnostics based on electrochemical transduction due to the excellent electrocatalytic properties of PBNPs towards a wide class of species based on reduction and oxidation processes. First, PBNPs–CMC hydrogel was drop casted on the working electrode of SPEs and the platform has been interrogated in presence of hydrogen peroxide. This is a very important analyte to be detected because it is one of the by–products of the oxidase enzymes: it means it can be used to indirectly quantify glucose, cholesterol, lactate and ethanol, if used in combination with glucose, cholesterol, lactate

and alcohol oxidase, respectively. The role of PBNPs toward the reduction of hydrogen peroxide is well–known in literature, although their catalytic performances are significantly affected by the shape and dimensions of the PB nanostructures [44]. On this regard, we have compared the electrocatalytic properties of SPEs modified with the newly synthesized PBNPs–CMC (DS 1.2) and with the hydrogel composite obtained by using CMC with lower DS, the PBNPs–CMC (DS 0.9), because the PBNPs associated with these hydrogels have different sizes. The electrocatalytic current for the reduction of H_2O_2 by the SPEs modified with the PBNPs–CMC (DS 1.2) is about 1.7 times higher than the current obtained from the PBNPs–CMC (DS 0.9) modified electrodes (Fig. S7). The higher catalytic activity can be ascribed to the smaller PBNPs (15 nm) entrapped in the PBNPs–CMC (DS 1.2) hydrogel. Moreover, significant differences on the adhesion properties of the two hydrogel films on the electrodes were observed. Indeed, a slow delamination of the PBNPs–CMC (DS 0.9) film from the electrode was observed upon a few drying—wetting cycles of the hydrogel film. On the contrary, the PBNPs–CMC (DS 1.2) hydrogel films show more strong adhesion properties on electrodes resulting in higher stability of the fabricated sensors (see below for the long-term stability test), as a consequence of the higher content of carboxylate groups on the CMC. Therefore, in this work only PBNPs–CMC obtained by using CMC with DS 1.2 is employed for the fabrication of the electrochemical (bio)sensors, because of the enhanced electrocatalytic properties and stability of these films on the electrode surface.

To optimize the sensing performances of the modified electrodes, we examined the effect of the volume of PBNPs–CMC hydrogel drop casted on the electrode surface. The thickness of the films, measured after swelling the hydrogel films in the electrolytic solution, increases from 79 μm to 182 μm as the volume of hydrogel drop casted on the electrode increases from 2 μl to 8 μl (Fig. 4). The swelled films adhere to the electrode surface until a limiting thickness is reached. In fact, when a volume of 12 μl is drop casted on the electrode, resulting in a film thickness of 223 μm, the film spontaneously delaminates from the surface upon drying.

The sensing performances of SPEs modified with different volumes of PBNPs–CMC hydrogel were evaluated through electrocatalytic reduction of 0.5 mM hydrogen peroxide. The catalytic current increases with the volume of hydrogel drop casted on the SPE and a plateau value is reached for the electrode modified with 6 μl of hydrogel, which is therefore considered as the optimal volume for the modification of the SPEs. In addition, an applied electrochemical potential of − 0.1 V (vs. Ag/AgCl) was determined as optimal for H_2O_2 detection (Fig. S8), in agreement with the value reported previously for other PB−modified electrodes [18]. As shown in Fig. 5A, the PBNPs–CMC modified electrodes have been applied towards the detection of hydrogen peroxide in standard solutions. The detection of hydrogen peroxide was satisfactory reaching very low limit of detection equal to ca. 50 μM and a

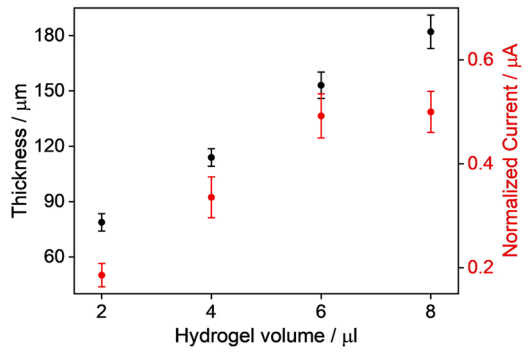

Fig. 4. Thickness of PBNPs−CMC films (black dots) and electrocatalytic current for the detection of 0.5 mM H_2O_2 solution (red dots) of PBNPs−CMC films obtained by drop casting of different hydrogel volumes on SPEs (diameter 4 mm).

repeatability of ca. 12%. It should be noted that the dynamic range of the platform was extended up to 2 mM hydrogen peroxide (Fig. S9).

Following these good results, the hydrogel composite also integrating glucose oxidase, the PBNPs−GOx−CMC, was employed for the modification of the printed strip to realize an electrochemical biosensor for the quantification of glucose in phosphate buffer solutions and serum samples as the model application.

As reported in Fig. 5B and Fig. S10, glucose was detected up to 20 mM and a 5 min−time of reaction was applied to allow the enzyme converting glucose and by−producing a detectable level of hydrogen peroxide. The calibration curves for glucose in buffer (Fig. S10) and in serum (Fig. 5B) show comparable sensitivity and dynamic range. This result suggests that there was not a significant effect from the matrix of the serum on the sensing performance, which can be ascribed to the ability of the CMC-based hydrogel film to minimize the nonspecific adsorption of proteins from biological fluids. The equation describing the determination of glucose in serum sample is $y = 0.024\ x - 0.006$ ($R^2 = 0.95$), where y indicates the signal difference between PBNPs−GOx−CMC modified SPE in presence of glucose and in absence of glucose, reported as μA, and x indicates the mM level of glucose. A detection limit of 1 mM was calculated, resulting in a ca. 3 mM as the quantification limit in serum samples.

The development of the biosensor for glucose demonstrates the biocompatibility of the conditions employed during the fabrication of the hydrogel films, in which the enzymes are retained in their catalytically active form. Our method revealed good reproducibility with a variability among different sensors < 10 %; this can be related to the approach for the preparation of the hydrogel composite, resulting in well-dispersed PBNPs and enzymes, and to the formation of homogeneous and stable hydrogel films on the electrode. The ability of the hydrogel composite to form stable films on the electrode surface and to preserve the activity of the embedded enzymes was tested by investigating the long–term stability of the PBNPs−GOx−CMC modified SPEs. We find that the biosensors retained > 90 % of the initial current response to 10 mM glucose after six–month storage at 4 °C (Fig. S11), indicating the good stability and robustness of our biosensors.

3.3. NADH and ethanol sensing

The PBNPs–CMC modified SPEs were then tested for the electrochemical detection of NADH, that is a coenzyme for many dehydrogenases, being involved in a wide range of enzymatic reactions [45]. In particular, we found the PBNPs embedded on the hydrogel films to be capable to catalyze the oxidation of NADH at low potentials, which represents an added point towards the analysis of real samples. As shown in Fig. 6A, the PBNPs–CMC modified SPEs have been interrogated in presence of different concentrations of NADH in buffer, using chronoamperometric detection with an applied potential of 0.4 V (vs. Ag/AgCl), chosen as the optimal potential for NADH oxidation (Fig. S12). The platform showed a linearity up to 200 μM of NADH described by the following equation, $y = 2.64\ x + 0.01$ ($R^2 = 0.99$), where y indicates the signal difference between the currents at different concentrations of NADH and the blank current, reported as μA, and x indicates the mM level of NADH. A detection limit of ca. 7 μM and a limit of quantification of ca. 20 μM has been determined for the NADH sensor. The mean repeatability of the method, calculated by considering the RSD due to three replicates using 20 μM NADH, was 9 %. In order to evaluate the response in a biological matrix, serum samples were spiked with increasing amounts of NADH as reported in Fig. 6B. Due to the presence of a more complex matrix, the sensitivity of the system slightly decreased with a slope of 1.77 μA/mM, but it should be noted that the decrease of sensitivity was limited by the presence of the CMC network.

NADH is the by–product of dehydrogenase enzymes, including alcohol dehydrogenase (ADH), which is widely used to develop biosensors for ethanol detection in food and pharmaceutical industries but also in the clinical setting [46]. Therefore, an electrochemical biosensor

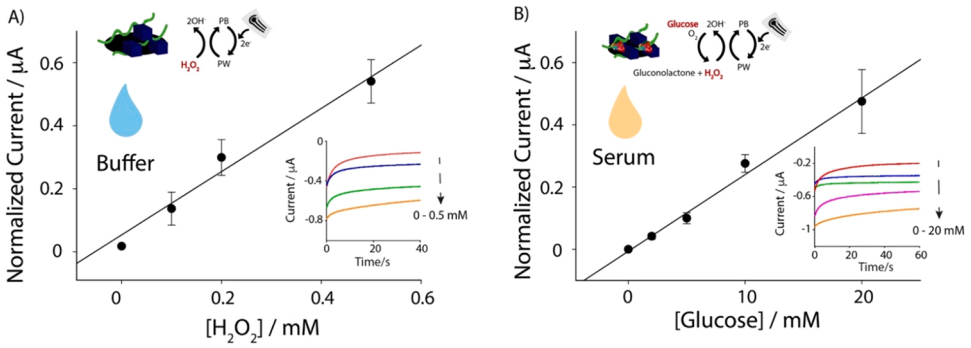

Fig. 5. A) Calibration curve obtained with increasing concentrations of hydrogen peroxide on PBNPs−CMC modified SPE in 0.05 M phosphate buffer at pH 7.4 with 150 mM KCl. Inset: chronoamperometric curves at − 0.1 V (vs. Ag/AgCl). B) Calibration curve obtained with increasing concentrations of glucose on PBNPs−GOx−CMC modified SPE in human serum samples. Inset: chronoamperometric curves at − 0.1 V (vs. Ag/AgCl).

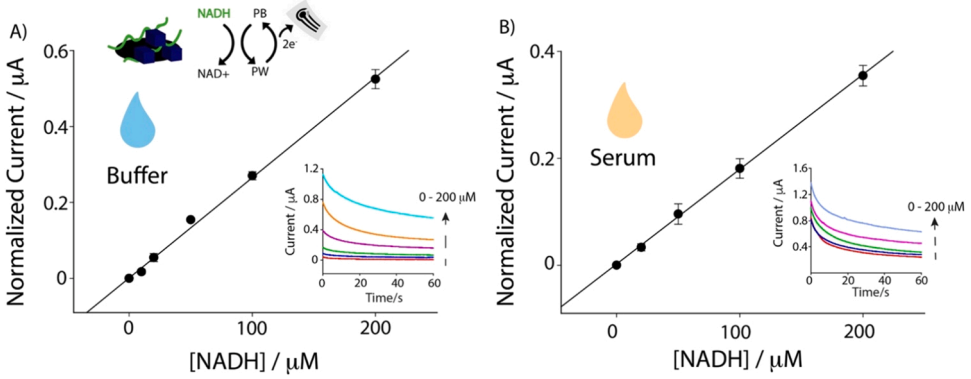

Fig. 6. A) Calibration curve obtained with increasing concentrations of NADH on PBNPs−CMC modified SPE in 0.05 M HEPES buffer at pH 7.0. Inset: chronoamperometric curves at 0.4 V (vs. Ag/AgCl). B) Calibration curve obtained with increasing concentrations of NADH in human serum samples. Inset: chronoamperometric curves at 0.4 V (vs. Ag/AgCl).

for ethanol was developed by modifying an electrochemical strip with the hydrogel composite integrating ADH, the PBNPs−ADH−CMC. The detection of ethanol by exploiting ADH enzyme is based on the catalytic conversion of ethanol to acetaldehyde in presence of NAD^+ that is reduced to NADH. Following this mechanism, ethanol can be indirectly quantified by monitoring the electrocatalytic oxidation of NADH on the modified electrode. As shown in Fig. 7A and B, the PBNPs−ADH−CMC modified SPE has been applied towards the detection of various levels of ethanol in both buffer solution and serum. The PBNPs−ADH−CMC modified SPEs have been interrogated in presence of ethanol up to 10 mM, using chronoamperometric detection according to the optimized conditions obtained for NADH measurements. The analysis of ethanol in buffer and serum displayed a linearity up to 10 mM, described by the following equations, $y = 0.05\ x - 0.01$ ($R^2 = 0.98$) and $y = 0.02\ x - 0.01$ ($R^2 = 0.96$), respectively, where y indicates the signal difference between the currents at different concentrations of ethanol and the blank current reported as µA, and x indicates the mM level of ethanol. The analysis of ethanol in serum samples was characterized by a detection limit of 0.3 mM, a quantification limit of ca. 1 mM, and a RSD of 11 %.

3.4. Comparison of analytical performances

The developed electrochemical biosensors have been well-compared

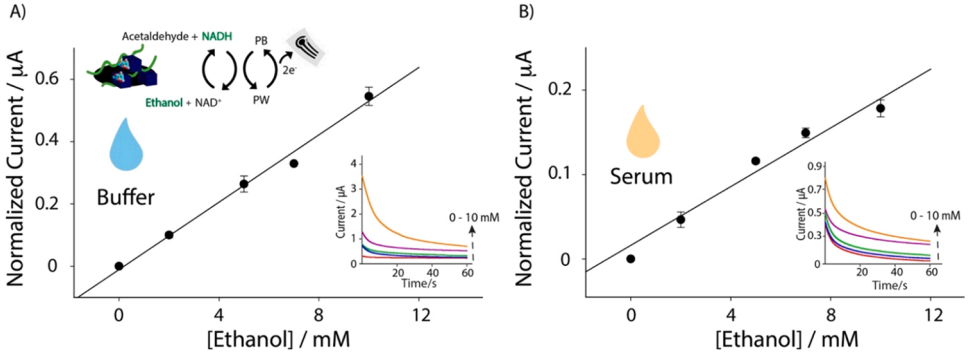

Fig. 7. A) Calibration curve obtained with increasing concentrations of ethanol on PBNPs−ADH−CMC modified SPE in 0.05 M HEPES buffer at pH 7.0 in the presence of 5 mM NAD^+. Inset: chronoamperometric curves at 0.4 V (vs. Ag/AgCl). B) Calibration curve obtained with increasing concentrations of ethanol in human serum samples. Inset: chronoamperometric curves at 0.4 V (vs. Ag/AgCl).

in terms of analytical performances with other electrochemical platforms reported in literature for the detection of NADH, ethanol and glucose, based on Prussian Blue and other NPs. With regards to NADH detection, the use of a nanocomposite made with PB–rGO yielded a detection limit of 68.4 μM [47], while the implementation of graphene–Au nanorods nanocomposites allowed to detect 6 μM as the lower limit [48]. Prussian Blue bulk-modified SPEs were also used to detect NADH in combination with NADH oxidase reaching a detection limit of ca. 0.11 μM by employing a flow injection analysis setting [14]. NADH has been also used to indirectly detect ethanol by different architectures; for example, an amperometric biosensor based on the ADH has been developed to detect ethanol in ethanol-methanol mixtures exploiting Meldola Blue as redox mediator, reaching a detection limit of 15 mM [49]. Pingarrón and co-workers employed MWCNTs, AuNPs, and ADH, in presence of its cofactor NAD^+, to develop an electrochemical biosensor to quantify ethanol down to 4.7 μM [50].

The analytical performance of our PBNPs−GOx−CMC biosensor toward the detection of glucose also demonstrated good agreement with the literature. For example, PB synthesized onto chromatographic paper allowed a ca. 1 mM detection limit of glucose in blood [18], while the use of polypyrrole/PB modified with Ni–hexacyanoferrates resulted in a 0.15 mM detection limit [51]. Electrodes modified with composite materials have been employed for the fabrication of glucose biosensors. Among them, a composite of graphene aerogel and Prussian Blue, prepared via chemical reduction through a freeze-drying process, has been used for the modification of SPEs followed by immobilization of GOx in a chitosan matrix: this multi-step fabrication process resulted in a glucose biosensor with a detection limit down to 0.15 mM [52]. It is evident how multiple architectures can be utilized to detect glucose, ethanol or NADH, however a simple approach as the one reported in this work highlights the ability to develop a versatile one–pot platform to be coupled to various sensing and biosensing devices.

4. Conclusion

In conclusion, we have developed a facile strategy for the preparation of electrochemical biosensors by modifying flexible screen–printed electrodes with porous hydrogel composites. The hydrogel network is obtained under biocompatible one–pot reaction conditions resulting in the formation of PBNPs and the simultaneous immobilization of enzymes and NPs in the matrix. The polymer chains, based on highly functionalized carboxymethyl cellulose, act as templating agents for the synthesis of size–controlled crystalline PBNPs and as gelator to generate an hydrogel network that can be easily drop casted on electrode surfaces to obtain stable and homogeneous films. The obtained hydrogel film-modified electrodes, therefore, can be directly employed for the development of electrochemical biosensors for the detection of a variety of analytes. Indeed, the electrochemical properties of the PBNPs can be switched between the application of oxidative and reducing potentials in order to quantify NADH and hydrogen peroxide, respectively. When the hydrogel–based synthesis of PBNPs is performed in the presence of enzymes, i.e. alcohol dehydrogenase and glucose oxidase, it is possible to fabricate an integrated enzyme-PBNPs hydrogel film on the electrode. The porous hydrogel membrane allows an efficient diffusion of ethanol on the ADH and of glucose on the GOx embedded in the films and the generated NADH/H_2O_2 is electrocatalytically oxidized/reduced on the PBNPs leading to the anodic/cathodic current respectively. The presence of the polymer scaffold protects the PBNPs and enzymes from leakage and degradation, increasing the durability of the sensing device, and stabilizes its response when employed in biological complex media.

Therefore, our approach holds great promise for the development of novel electrochemical (bio)sensors, which are easy to obtain, cheap and versatile. The developed hydrogel films with their robust crosslinked network and high loading capacity can favor the simultaneous immobilization of NPs and different enzymes, in order to expand the number of analytes to determine using a single platform, and provides also a protective and flexible scaffold to increase the robustness of the electrochemical biosensors which is required for point–of–need applications.

Funding details

This research was supported by the University of Padova under the 2019 STARS Grant programme “SensCo”.

CRediT authorship contribution statement

Roberto Baretta: Investigation, Data curation, Visualization, Writing-Review & Editing, Formal analysis. **Ada Raucci:** Investigation, Data curation, Visualization, Formal analysis. **Stefano Cinti:** Methodology, Validation, Writing-Original Draft, Funding acquisition, Visualization, Supervision, Resources. **Marco Frasconi:** Conceptualization, Methodology, Writing-Original Draft, Funding acquisition, Visualization, Supervision, Resources.

Declaration of Competing Interest

The authors declare that they have no known competing financial interests or personal relationships that could have appeared to influence the work reported in this paper.

Data Availability

Data will be made available on request. Data available by request to the corresponding authors.

Acknowledgements

We would like to acknowledge Dr Andrea Basagni (University of Padova) for help with SEM characterization.

Appendix A. Supporting information

Supplementary data associated with this article can be found in the online version at doi:10.1016/j.snb.2022.132985.

References

[1] H. Golmohammadi, E. Morales-Narváez, T. Naghdi, A. Merkoçi, Nanocellulose in sensing and biosensing, Chem. Mater. 29 (2017) 5426–5446, https://doi.org/10.1021/acs.chemmater.7b01170.
[2] J.D. Mota-Morales, E. Morales-Narváez, Transforming nature into the next generation of bio-based flexible devices: new avenues using deep eutectic systems, Matter 4 (2021) 2141–2162, https://doi.org/10.1016/j.matt.2021.05.009.
[3] X. Sun, S. Agate, K.S. Salem, L. Lucia, L. Pal, Hydrogel-based sensor networks: compositions, properties, and applications - a review, ACS Appl. Bio Mater. 4 (2021) 140–162, https://doi.org/10.1021/acsabm.0c01011.
[4] R. Ajdary, B.L. Tardy, B.D. Mattos, L. Bai, O.J. Rojas, Plant nanomaterials and inspiration from nature: water interactions and hierarchically structured hydrogels, Adv. Mater. 33 (2021), 2001085, https://doi.org/10.1002/adma.202001085.
[5] M. Vázquez-González, I. Willner, Stimuli-responsive biomolecule-based hydrogels and their applications, Angew. Chem. Int. Ed. 59 (2020) 15342–15377, https://doi.org/10.1002/anie.201907670.
[6] J.Y.C. Lim, S.S. Goh, X.J. Loh, Bottom-up engineering of responsive hydrogel materials for molecular detection and biosensing, ACS Mater. Lett. 2 (2020) 918–950, https://doi.org/10.1021/acsmaterialslett.0c00204.
[7] L. Ionov, Hydrogel-based actuators: possibilities and limitations, Mater. Today 17 (2014) 494–503, https://doi.org/10.1016/j.mattod.2014.07.002.
[8] A. Herrmann, R. Haag, U. Schedler, Hydrogels and their role in biosensing applications, Adv. Healthc. Mater. 10 (2021), 2100062, https://doi.org/10.1002/adhm.202100062.
[9] E. Nicol, Photopolymerized porous hydrogels, Biomacromolecules 22 (2021) 1325–1345, https://doi.org/10.1021/acs.biomac.0c01671.
[10] J. Zhang, J. Jin, J. Wan, S. Jiang, Y. Wu, W. Wang, X. Gong, H. Wang, Quantum dots-based hydrogels for sensing applications, Chem. Eng. J. 408 (2021), 127351, https://doi.org/10.1016/j.cej.2020.127351.
[11] A.Sinha Dhanjai, P.K. Kalambate, S.M. Mugo, P. Kamau, J. Chen, R. Jain, Polymer hydrogel interfaces in electrochemical sensing strategies: a review, TrAC - Trends Anal. Chem. 118 (2019) 488–501, https://doi.org/10.1016/j.trac.2019.06.014.

[12] D. Zhai, B. Liu, Y. Shi, L. Pan, Y. Wang, W. Li, R. Zhang, G. Yu, Highly sensitive glucose sensor based on Pt nanoparticle/polyaniline hydrogel heterostructures, ACS Nano 7 (2013) 3540–3546, https://doi.org/10.1021/nn400482d.
[13] A. Cioffi, M. Mancini, V. Gioia, S. Cinti, Office paper-based electrochemical strips for organophosphorus pesticide monitoring in agricultural soil, Environ. Sci. Technol. 55 (2021) 8859–8865, https://doi.org/10.1021/acs.est.1c01931.
[14] A. Radoi, D. Compagnone, E. Devic, G. Palleschi, Low potential detection of NADH with Prussian Blue bulk modified screen-printed electrodes and recombinant NADH oxidase from Thermus thermophilus, Sens. Actuators B Chem. 121 (2007) 501–506, https://doi.org/10.1016/j.snb.2006.04.075.
[15] L. Yu, J. Zhao, S. Tricard, Q. Wang, J. Fang, Efficient detection of ascorbic acid utilizing molybdenum oxide@Prussian Blue/graphite felt composite electrodes, Electrochim. Acta 322 (2019), 134712, https://doi.org/10.1016/j.electacta.2019.134712.
[16] S. Salatiello, M. Spinelli, C. Cassiano, A. Amoresano, F. Marini, S. Cinti, Sweat urea bioassay based on degradation of Prussian Blue as the sensing architecture, Anal. Chim. Acta 1210 (2022), 339882, https://doi.org/10.1016/j.aca.2022.339882.
[17] A.A. Karyakin, E.E. Karyakina, Prussian Blue-based "artificial peroxidase" as a transducer for hydrogen peroxide detection. Application to biosensors, Sens. Actuators B Chem. 57 (1999) 268–273, https://doi.org/10.1016/S0925-4005(99)00154-9.
[18] S. Cinti, R. Cusenza, D. Moscone, F. Arduini, Paper-based synthesis of Prussian Blue Nanoparticles for the development of whole blood glucose electrochemical biosensor, Talanta 187 (2018) 59–64, https://doi.org/10.1016/j.talanta.2018.05.015.
[19] S. Cinti, F. Arduini, D. Moscone, G. Palleschi, L. Gonzalez-Macia, A.J. Killard, Cholesterol biosensor based on inkjet-printed Prussian blue nanoparticle-modified screen-printed electrodes, Sens. Actuators B Chem. 221 (2015) 187–190, https://doi.org/10.1016/j.snb.2015.06.054.
[20] J. Kim, I. Jeerapan, S. Imani, T.N. Cho, A. Bandodkar, S. Cinti, P.P. Mercier, J. Wang, Noninvasive alcohol monitoring using a wearable tattoo-based iontophoretic-biosensing system, ACS Sens. 1 (2016) 1011–1019, https://doi.org/10.1021/acssensors.6b00356.
[21] M.A. Komkova, A.A. Eliseev, A.A. Poyarkov, E.V. Daboss, P.V. Evdokimov, A. A. Eliseev, A.A. Karyakin, Simultaneous monitoring of sweat lactate content and sweat secretion rate by wearable remote biosensors, Biosens. Bioelectron. 202 (2022), 113970, https://doi.org/10.1016/j.bios.2022.113970.
[22] M.C. Hartel, D. Lee, P.S. Weiss, J. Wang, J. Kim, Resettable sweat-powered wearable electrochromic biosensor, Biosens. Bioelectron. 215 (2022), 114565, https://doi.org/10.1016/j.bios.2022.114565.
[23] J.R. Sempionatto, M. Lin, L. Yin, E. De la paz, K. Pei, T. Sonsa-ard, A.N. de Loyola Silva, A.A. Khorshed, F. Zhang, N. Tostado, S. Xu, J. Wang, An epidermal patch for the simultaneous monitoring of haemodynamic and metabolic biomarkers, Nat. Biomed. Eng. 5 (2021) 737–748, https://doi.org/10.1038/s41551-021-00685-1.
[24] S. Ying, C. Chen, J. Wang, C. Lu, T. Liu, Y. Kong, F.Y. Yi, Synthesis and applications of Prussian Blue and its analogues as electrochemical sensors, ChemPlusChem 86 (2021) 1608–1622, https://doi.org/10.1002/cplu.202100423.
[25] M. Wang, X. Kan, Multilayer sensing platform: gold nanoparticles/Prussian Blue decorated graphite paper for NADH and H_2O_2 detection, Analyst 143 (2018) 5278–5284, https://doi.org/10.1039/c8an01502c.
[26] F. Ricci, G. Palleschi, Sensor and biosensor preparation, optimisation and applications of Prussian Blue modified electrodes, Biosens. Bioelectron. 21 (2005) 389–407, https://doi.org/10.1016/j.bios.2004.12.001.
[27] M. Shokouhimehr, E.S. Soehnlen, J. Hao, M. Griswold, C. Flask, X. Fan, J. P. Basilion, S. Basu, S.D. Huang, Dual purpose Prussian Blue nanoparticles for cellular imaging and drug delivery: a new generation of T1-weighted MRI contrast and small molecule delivery agents, J. Mater. Chem. 20 (2010) 5251–5259, https://doi.org/10.1039/b923184f.
[28] Z. Qin, B. Chen, Y. Mao, C. Shi, Y. Li, X. Huang, F. Yang, N. Gu, Achieving ultrasmall Prussian Blue Nanoparticles as high-performance biomedical agents with multifunctions, ACS Appl. Mater. Interfaces 12 (2020) 57382–57390, https://doi.org/10.1021/acsami.0c18357.
[29] S. Eun, H.J. Hong, H. Kim, H.S. Jeong, S. Kim, J. Jung, J. Ryu, Prussian Blue-embedded carboxymethyl cellulose nanofibril membranes for removing radioactive cesium from aqueous solution, Carbohydr. Polym. 235 (2020), 115984, https://doi.org/10.1016/j.carbpol.2020.115984.
[30] R. Baretta, V. Gabrielli, M. Frasconi, Nanozyme−cellulose hydrogel composites enabling cascade catalysis for the colorimetric detection of glucose, ACS Appl. Nano Mater. 5 (2022) 13845–13853, https://doi.org/10.1021/acsanm.2c01609.
[31] H. Orelma, T. Teerinen, L.S. Johansson, S. Holappa, J. Laine, CMC-modified cellulose biointerface for antibody conjugation, Biomacromolecules 13 (2012) 1051–1058, https://doi.org/10.1021/bm201771m.
[32] A. Raucci, A. Miglione, M. Spinelli, A. Amoresano, S. Cinti, A hybrid screen-printed strip for enhanced electroanalysis towards lead and cadmium in multi-matrices, J. Electrochem. Soc. 169 (2022), 037516, https://doi.org/10.1149/1945-7111/ac5c98.
[33] V. Gabrielli, R. Baretta, R. Pilot, A. Ferrarini, M. Frasconi, Insights into the gelation mechanism of metal-coordinated hydrogels by paramagnetic NMR spectroscopy and molecular dynamics, Macromolecules 55 (2022) 450–461, https://doi.org/10.1021/acs.macromol.1c01756.
[34] L. Catala, T. Mallah, Nanoparticles of Prussian Blue analogs and related coordination polymers: from information storage to biomedical applications, Coord. Chem. Rev. 346 (2017) 32–61, https://doi.org/10.1016/j.ccr.2017.04.005.
[35] C. Wang, M. Fadeev, M. Vázquez-González, I. Willner, Stimuli-responsive donor–acceptor and DNA-crosslinked hydrogels: application as shape-memory and self-healing materials, Adv. Funct. Mater. 28 (2018), 1803111, https://doi.org/10.1002/adfm.201803111.
[36] M. Vázquez-González, R.M. Torrente-Rodríguez, A. Kozell, W.C. Liao, A. Cecconello, S. Campuzano, J.M. Pingarrón, I. Willner, Mimicking peroxidase activities with Prussian Blue nanoparticles and their cyanometalate structural analogues, Nano Lett. 17 (2017) 4958–4963, https://doi.org/10.1021/acs.nanolett.7b02102.
[37] H.J. Buser, D. Schwarzenbach, W. Petter, A. Ludi, The crystal structure of Prussian Blue: $Fe_4[Fe(CN)_6]_3 \times H_2O$, Inorg. Chem. 16 (1977) 2704–2710, https://doi.org/10.1021/ic50177a008.
[38] E. Jin, X. Lu, L. Cui, D. Chao, C. Wang, Fabrication of graphene/Prussian Blue composite nanosheets and their electrocatalytic reduction of H_2O_2, Electrochim. Acta 55 (2010) 7230–7234, https://doi.org/10.1016/j.electacta.2010.07.029.
[39] P. Zhou, D. Xue, H. Luo, X. Chen, Fabrication, structure, and magnetic properties of highly ordered Prussian Blue nanowire arrays, Nano Lett. 2 (2002) 845–847, https://doi.org/10.1021/nl0256154.
[40] K. Feng, J. Zhang, H. Dong, Z. Li, N. Gu, M. Ma, Y. Zhang, Prussian Blue Nanoparticles having various sizes and crystallinities for multienzyme catalysis and magnetic resonance imaging, ACS Appl. Nano Mater. 4 (2021) 5176–5186, https://doi.org/10.1021/acsanm.1c00617.
[41] F. Ricci, C. Gonçalves, A. Amine, L. Gorton, G. Palleschi, D. Moscone, Electroanalytical study of Prussian Blue modified glassy carbon paste electrodes, Electroanalysis 15 (2003) 1204–1211, https://doi.org/10.1002/elan.200390148.
[42] B. Haghighi, H. Hamidi, L. Gorton, Electrochemical behavior and application of Prussian Blue nanoparticle modified graphite electrode, Sens. Actuators B Chem. 147 (2010) 270–276, https://doi.org/10.1016/j.snb.2010.03.020.
[43] A.L. Eckermann, D.J. Feld, J.A. Shaw, T.J. Meade, Electrochemistry of redox-active self-assembled monolayers, Coord. Chem Rev. 254 (2010) 1769–1802, https://doi.org/10.1016/j.ccr.2009.12.023.
[44] S. Cinti, F. Arduini, G. Vellucci, I. Cacciotti, F. Nanni, D. Moscone, Carbon black assisted tailoring of Prussian Blue nanoparticles to tune sensitivity and detection limit towards H_2O_2 by using screen-printed electrode, Electrochem. Commun. 47 (2014) 63–66, https://doi.org/10.1016/j.elecom.2014.07.018.
[45] A. Radoi, D. Compagnone, Recent advances in NADH electrochemical sensing design, Bioelectrochemistry 76 (2009) 126–134, https://doi.org/10.1016/j.bioelechem.2009.06.008.
[46] P.D. Thungon, A. Kakoti, L. Ngashangva, P. Goswami, Advances in developing rapid, reliable and portable detection systems for alcohol, Biosens. Bioelectron. 97 (2017) 83–99, https://doi.org/10.1016/j.bios.2017.05.041.
[47] S. Immanuel, R. Sivasubramanian, Electrochemical kinetic investigation of NADH oxidation on Prussian Blue-mediated chemically reduced graphene oxide nanosheets, J. Phys. Chem. Solids 161 (2022), 110471, https://doi.org/10.1016/j.jpcs.2021.110471.
[48] L. Li, H. Lu, L. Deng, A sensitive NADH and ethanol biosensor based on graphene-Au nanorods nanocomposites, Talanta 113 (2013) 1–6, https://doi.org/10.1016/j.talanta.2013.03.074.
[49] B. Bucur, G.L. Radu, C.N. Toader, Analysis of methanol-ethanol mixtures from falsified beverages using a dual biosensors amperometric system based on alcohol dehydrogenase and alcohol oxidase, Eur. Food Res. Technol. 226 (2008) 1335–1342, https://doi.org/10.1007/s00217-007-0662-4.
[50] J. Manso, M.L. Mena, P. Yáñez-Sedeño, J.M. Pingarrón, Alcohol dehydrogenase amperometric biosensor based on a colloidal gold-carbon nanotubes composite electrode, Electrochim. Acta 53 (2008) 4007–4012, https://doi.org/10.1016/j.electacta.2007.10.003.
[51] A.I. Rekertaitė, A. Valiūnienė, P. Virbickas, A. Ramanavicius, Physicochemical characteristics of polypyrrole/(glucose oxidase)/(Prussian Blue)-based biosensor modified with Ni- and Co-hexacyanoferrates, Electroanalysis 31 (2019) 50–57, https://doi.org/10.1002/elan.201800526.
[52] T. Hu, D. Wang, J. Xu, K. Chen, X. Li, H. Yi, Z. Ni, Glucose sensing on screen-printed electrochemical electrodes based on porous graphene aerogel @Prussian Blue, Biomed. Micro 24 (2022) 14, https://doi.org/10.1007/s10544-022-00614-2.

Roberto Baretta is a first year Ph.D. student in Molecular Sciences at University of Padova, Department of Chemical Sciences. His research interests focus on the development of stimuli-responsive hydrogels and polymer films for biosensing applications.

Ada Raucci is a first year Ph.D. student in Pharmaceutical Science at the Department of Pharmacy at University of Naples Federico II. Her research is mainly focused on the development of electrochemical (bio)sensors for determining emerging pollutants in agri-food, environmental, and clinical samples. Her fields of interests are porous materials, wearable, screen-printing and nanomaterials.

Stefano Cinti is an Associate Professor at the Department of Pharmacy, University of Naples "Federico II" and he leads the uninanobiosensors Lab (uninanobiosensors.com). His research interests include the development of electrochemical sensors, paper-based devices, nanomotors, and nanomaterials. During his research activity, he had the opportunity to spend a period abroad in Finland, U.K., U.S., Germany, and Spain. He has published more than 60 papers in peer-reviewed journals, with an H-index of 28 and > 2800 citations. Among all the prizes and certificates, in 2018 he was named Best Young Researcher in Bio-Analytical Chemistry, and in 2019 he was named Best Young Researcher in Analytical Chemistry (Italian Chemical Society), and in 2021 he has been recognized as the World's Top 2% Scientists. He is the coordinator of Chemical Cultural Diffusion group and he is the Chair of AMYC-BIOMED, a multidisciplinary conference for young chemists in the biomedical sciences.

Marco Frasconi is Associate Professor of Analytical Chemistry at University of Padova, Department of Chemical Sciences. He received his Ph.D. in 2010 from University of Rome "Sapienza". He was a Postdoctoral research fellow at Northwestern University (2010-2014) and at the Italian Institute of Technology (2014-2015). His research interests focus on supramolecular chemistry, biomimetic materials, nano-bio interfaces, electrochemical biosensors and stimuli-responsive hydrogels.